Automatic Property Identification
via Parameterized Constraints

Thomas Debus and Pierre Dupont

Robert Howe

Aerospace and Mechanical Engineering
Boston University
Boston, MA 02215

Division of Applied Science
Harvard University
Cambridge, MA 02138

Abstract— During teleoperation, the automatic identification of remote environment properties has the potential of improving performance by providing task-specific feedback to the operator. Similarly, virtual training systems can be calibrated using such an automatic identification procedure. For those properties which can be described by parameterized constraint equations, this paper provides a method by which the active constraints can be determined during each portion of the remote manipulator's data stream. The parameterized properties can then be estimated from the appropriate data stream segments. The approach is validated for peg-in-hole insertion using a desktop teleoperator system. The proposed segmentation procedure is compared with manual segmentation to estimate the geometric properties of the peg and hole.

Index Terms- telemanipulators, property identification, constrained motion.

I. INTRODUCTION

In current teleoperation applications, the operator is responsible for interpreting sensor feedback from the remote manipulator. Subsequent manipulation strategies are based on this interpretation. In many cases, however, machine perception of the remote environment could enhance the operator's perception of the environment and thereby dramatically improve task performance. For example, in remediation of toxic waste dumps, quantitative measurements of the size and weight of the containers helps to infer their contents and to determine optimal handling strategies [9]. Additional application areas include undersea mining and salvage, interplanetary exploration, and the defusing of explosives.

In critical applications such as these, effective operator training is a significant concern. To address this need, machine perception can also be used to develop and calibrate models of the environment for use as real-time simulators and training systems. Training systems calibrated using actual feedback data would provide a realistic and safe practice environment for surgical applications [17], toxic waste remediation [9], and munitions loading [11]. In contrast, current methods to calibrate virtual models typically rely on subjective hand tuning of simplified physical models. Exceptions to this include the work of Dupont and co-workers [5], [6] and MacLean [13], in which force-displacement data is used to recreate the haptic sensations of manipulating virtual objects.

A general framework for solving the automatic property identification problem was proposed in [6]. This framework reduces the solution to solving three subproblems: task decomposition, data segmentation, and property estimation. The contribution of this paper is to provide a unified solution procedure to the segmentation and estimation subproblems for those properties which affect the contact between a manipulated object and the remote environment. This includes, for example, the contact geometry of the workpiece and environment.

In the next section, the property identification solution framework of [6] is summarized. The following section describes the segmentation and property estimation procedure developed for contact properties. Given the task decomposition, constraint equations describing the subtask contact states are developed, parameterized by the unknown contact properties. The set of active constraints at each instant is determined using multiple correlation coefficients. The desired properties can then be estimated using least squares.The subsequent section described an experimental evaluation of the approach using a tabletop teleoperator system. The geometric properties of a peg and hole are estimated during a planar insertion task. Conclusions are presented in the final section of the paper.

II. AUTOMATIC PROPERTY IDENTIFICATION

From [6], the identification problem can be formally defined as follows.

Given a task description, $\mathcal{T}$, a sensor data stream, $d(t)$, and a set of properties to be determined, p, compute estimates of the states, $\hat{x}(t)$, and the properties, $\hat{p}(t)$, for $t \in [0, t_{final}]$.

A *task description*, $\mathcal{T}$, contains, at a minimum, a specification of the desired interactions between objects in the remote environment. Additional detail could indicate which objects the robot should handle and available grasp configurations. It could also include parameterized models of objects relating to, e.g., geometry and contact forces.

State, $x(t)$, is defined by the manipulated object and a description of the set of active constraints between it and all other objects in the environment, including the remote manipulator. *Properties* estimated in the identification problem

are those of the manipulated objects and of those objects with which they have contact. The latter class includes the remote manipulator. Examples of such properties are shape, size, weight, mass distribution, stiffness and friction.

A. Solution Procedure

The following decomposition of the identification problem into the three subproblems of task decomposition, data segmentation and property estimation will be used here [5].

1. <u>Task decomposition</u> - the process of resolving a task $\mathcal{T}$ into a minimal sequence of *subtasks*, s_i, described by contact states and their associated sets of properties, $\mathcal{T} = \{s_1 = (x_1, p_1), s_2 = (x_2, p_2), \ldots, s_q = (x_q, p_q)\}$ where p_i, $i = 1, \ldots, r$, are subsets of p. Note that an individual state and/or property may be associated with multiple subtasks.

2. <u>Data segmentation</u> - Given a task decomposition $\mathcal{T} = \{s_1, s_2, \ldots, s_q\}$ and the sensor data stream $d(t)$, find the time intervals corresponding to each subtask, $\{(t_{1,i}, t_{1,f}), (t_{2,i}, t_{2,f}), \ldots, (t_{q,i}, t_{q,f})\}$. To allow for sensor noise as well as unanticipated states, it is not required that $t_{j,f} = t_{j+1,i}$. Since there is uncertainty in determining the time intervals, the jth interval provides only estimates of the subtask and state, $\hat{s}_j$ and $\hat{x}_j$, respectively. Data segmentation may be performed either on or off line. If performed on line, the estimates can be expressed as functions of time.

3. <u>Property estimation</u> - Given the time intervals $\{(t_{1,i}, t_{1,f}), (t_{2,i}, t_{2,f}), \ldots, (t_{q,i}, t_{q,f})\}$ associated with each subtask, estimate the desired properties, $\hat{p}$. If this procedure is carried out on line, the properties can be written as $\hat{p}(t)$.

The concept of the automatic environment identification system can be described as follow. As a normal teleoperated task is performed, the system collects such data as task descriptions and desired properties from the operator. The resulting forces and motions are received from sensors in the remote environment. Visual feedback, as well as interaction with the human operator and data segmentation module, may also be necessary to efficiently decompose the task into its constituent parts. Based on the deduced sequence of subtasks, the data segmentation module associates subtasks (and thus states) with time segments of the data stream. The desired properties are then estimated and used to build and calibrate a model of the remote environment. The model can then be used either to provide immediate assistance to the operator or to form the basis of a training system.

B. Prior Work

This paper focuses on the subproblems of data segmentation and property estimation. These topics have received attention in the literature, however, not in the context of property identification. For example, Pook and Ballard employed data segmentation in order to understand the quali-

tative control characteristics of an example task performed on a teleoperated system [16]. Delson and West used human demonstration to program robots and in the process had to segment the data into subtasks that facilitated the generation of a robot program [3]. Eberman employed estimation theory to build a contact state observer as a step toward autonomous manipulation [7].

Segmentation methods described in the literature include hidden Markov models [10], generalized likelihood ratio test [7], qualitative reasoning with thresholding [14], neural networks for off-line segmentation [8] and Petri nets [15].

Most work on property estimation assumes a parameterized model, e.g., a geometric or contact force model. A significant portion of this literature is devoted to robot parameter identification. For example, the identification of link inertial parameters has been studied by An et al. [1]. Others have investigated the identification of kinematic parameters [4]. In addition, a few authors have addressed identification of robot payload and environment properties. Methods for estimating payload inertia appear in the work of Lin and Yae [12]. Lin and Yae also estimate certain parameters relating to constraints of the operating environment. Constraint existence and modeling are studied in [5], and constraint parameter identification in [2].

III. CONTACT CONSTRAINT SEGMENTATION AND ESTIMATION

A model for the manipulated object (and contacting objects) can, in some cases, be derived from the task description. Alternatively, an object model can be inferred from visual and force/displacement data and updated as new data becomes available. Given a model, the properties will often correspond to specific model parameters. They can then be written as a vector of real numbers, $p \in \Re^m$. Their estimates, $\hat{p}(t)$ can be considered time dependent when estimation is performed on line.

In this paper, we assume that the task decomposition problem has been solved. Thus the input to the segmentation problem consists of the task description given by

$$\mathcal{T} = \{s_1 = (x_1, p_1), s_2 = (x_2, p_2), \ldots, s_q = (x_q, p_q)\} \quad (1)$$

in which the task $\mathcal{T}$ has been expressed as a minimal sequence of *subtasks*, s_i, described by contact states and their associated property subsets, p_i. For each subtask, the contact state descriptions, x_i, convey the relationship between the manipulated object and all the other objects in the environment.

Contact states, x_i, can be expressed as a set of pairs of parameterized constraint equations. Each pair is based on the feasible geometry of contact for the manipulated object and a particular object (or surface) in the environment. For example, point contact between the manipulated object and an environment object can be expressed as

$$f_j(X_c^m(t), Y_c^m(t), Z_c^m(t)) = 0$$
$$g_j(X_c^e(t), Y_c^e(t), Z_c^e(t)) = 0 \quad (2)$$

Here, f_j and g_j are vector-valued functions of the jth contact's coordinates written with respect to body frames of the manipulated object, (X_c^m, Y_c^m, Z_c^m), and the environment object, (X_c^e, Y_c^e, Z_c^e).

These functions are related through the kinematic closure equation

$$T_o^m(t)\begin{bmatrix} X_c(t) \\ Y_c(t) \\ Z_c(t) \\ 1 \end{bmatrix}^m = T_o^e(t)\begin{bmatrix} X_c(t) \\ Y_c(t) \\ Z_c(t) \\ 1 \end{bmatrix}^e \qquad (3)$$

in which $T_o^m(t)$ is a homogeneous transform matrix which relates the manipulated object body frame, through the remote manipulator's kinematics, to the remote environment base frame. Similarly, $T_o^e(t)$ relates the environment object body frame to the remote environment base frame. At any instant, these transform matrices are identical for all active constraints pairs of the form given by (2). If the environment object is not moving or deforming, the matrix T_o^e is independent of time.

Equations (2) and (3) are a parameterized description of a particular contact. The parameters in (2) relate to the geometry of the contacting objects. For example, it may be known that the manipulated object is a cylinder, but its length and radius are unknown parameters. Similarly, the environment object may be known to be planar, but its normal and location are unknown.

While it is assumed that the remote manipulator's configuration is known, $T_o^m(t)$ in (3) also depends on the possibly unknown grasp configuration of the manipulated object. In addition, the base frame location of the environment object may be unknown leading to additional free parameters in $T_o^e(t)$.

A sufficient number of constraints must be associated with a particular contact state in order to be able to solve for the contact parameters. In particular,

$$\sum_{j=1}^{k}\left\{\dim(f_j)+\dim(g_j)\right\}\geq 3 \qquad (4)$$

where k is the number of point contacts associated with the contact state. To see this, consider that, for n time samples, there are $6n+u$ unknowns and $3n$ equations in (3). The $6n$ unknowns are due to the point contact coordinates in the manipulated and environment object body frames. The remaining u correspond to constant parameters in $T_o^m(t)$ and T_o^e. The set of active constraint pairs of the form given by (2) must introduce at least $3n$ equations which leads to (4). Assuming that the constraints themselves also introduce v parameters, the number of time samples, n, must satisfy

$$n\geq u+v \qquad (5)$$

The resulting equations can be arranged in the usual form as a set of algebraic equations which are linear in the unknown parameters or their products.

$$\tau=\Phi\theta \qquad (6)$$

Least squares can be used to solve for the parameters. It is necessary that the trajectory be sufficiently exciting to preclude low row rank of Φ.

A. Statistical Segmentation and Property Estimation

Segmentation is based on a multiple correlation coefficient acceptance test for each contact constraint. Such testing is conducted when nonzero contact forces are detected. These forces are inferred from configuration error between the remote and master manipulator. The segmentation problem is solved in the following steps.

For each subtask, s_i:

1. Convert the state description x_i from the form of (2) and (3) to that of (6).
2. Solve the least squares problem for the parameter values using a moving data window of width n satisfying (5).
3. For each data window, use the estimated parameters, $\hat{\theta}$, to compute $\hat{\tau}=\Phi\hat{\theta}$. Compute the squared multiple correlation coefficient,

$$R^2=\frac{\sum_{j=1}^{n}(\tau_j-\hat{\tau}_j)^2}{\sum_{j=1}^{n}(\tau_j-\bar{\tau})^2}. \qquad (7)$$

4. If $R^2\geq\alpha$, accept the data window as corresponding to state x_i and thus, subtask s_i. The value of α can be selected for any desired value of $P_n(R^2\geq\alpha)$, that is, the probability that, if the measured variable τ_j is uncorrelated to the measured variables in Φ_j, the measurements $\{\tau_j,\Phi_j\}, j=1,\ldots,n$ would yield $R^2\geq\alpha$.
5. Estimate the parameter values over all accepted data windows. Using these values, solve for the property subset estimate, $\hat{p}_i$.
6. Substitute as needed the estimates of $\hat{p}_i$ into all remaining subtask state descriptions x_{i+1} to x_q, thereby decreasing the number of properties remaining to be estimated.

If, for the last subtask, only a single unestimated parameter remains, employ a threshold on standard deviation, $\sigma\leq\beta$, instead of correlation factor, in the acceptance test.

IV. EXPERIMENTAL EXAMPLE

A tabletop teleoperator system, composed of two PHAN-ToM® haptic devices is used to perform a planar peg-in-hole insertion task. A sketch of the system is shown in Fig. 1. Each device is a 3 degree of freedom manipulator. In order to accomplish the desired task, a gripper is added to the remote manipulator. The operator controls the master by manipulating a stylus attached through a passive spherical wrist. At each sample time, the forward kinematics are computed such that the position of the end effector with respect to the base frame is known. The workspace is roughly

a box of dimension 19.5 cm $\times$ 27 cm $\times$ 37.5 cm. Each device can exert a continuous tip force of 1.7 N, and a maximum force of 8.5 N can be achieved.
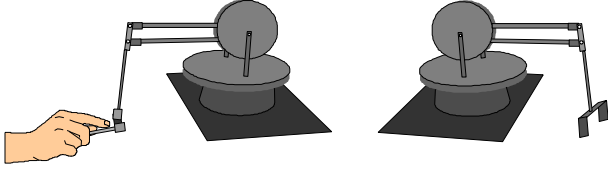

FIG. 1. Two PHANToM® haptic devices used as a teleoperator system.

The controller uses a symmetric proportional control scheme based on position and velocity error between the master and remote manipulators. See equation (8). The controller gains are adjusted experimentally to achieve stability and haptic realism. The controller output is taken as an estimate of the force acting on the robot's tip. The control loop rate is approximately 10 kHz.

$$F_i^{remote} = K_{pi}\left(X_i^{master} - X_i^{remote}\right) + K_{vi}\left(\dot{X}_i^{master} - \dot{X}_i^{remote}\right)$$
$$F_i^{master} = -F_i^{remote}, \quad i = \{x, y, z\} \tag{8}$$

A. Contact Constraints

During planar peg-in-hole insertion, four primary contact states can occur. These contact states are depicted in Fig. 2. By combining these primary contacts, multiple contact states can be created. In fact, any contact made during the insertion can be described by some combination of the four primary contacts.
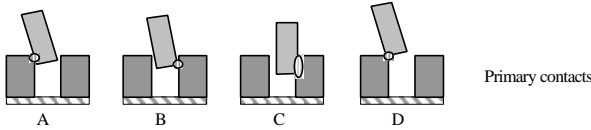

Primary contacts

Fig. 2. Primary Contact states.

The primary contacts can be described by equations of the form of (2) and (3). It is assumed that the body frame of the environment object (the hole) coincides with the remote environment base frame. Since the motion is planar, (3) reduces to

$$T_o^m(t) \begin{bmatrix} X_c(t) \\ Y_c(t) \\ 1 \end{bmatrix}^m = \begin{bmatrix} X_c(t) \\ Y_c(t) \\ 1 \end{bmatrix}^e \tag{9}$$

In order to express the primary contacts in the form given by (2), the following assumptions are made.

1. Once grasped, the peg does not slip in the gripper.
2. The constraints are holonomic.
3. The manipulated object (peg) is rectangular and one axis of its body frame is parallel to the sides of the peg.
4. The hole's axis is orthogonal to the surface in which it is drilled.

For each primary contact, equation (2) can be expressed as follows:

Contact A
$$X_c^m(t) - B = 0$$
$$X_c^e(t) + \alpha = 0$$
$$Y_c^e(t) + \beta = 0 \tag{10}$$

Contact B
$$X_c^m(t) + \delta = 0$$
$$Y_c^m(t) + \gamma = 0$$
$$X_c^e(t) - MY_c^e(t) - \rho = 0 \tag{11}$$

Contact D
$$X_c^m(t) + \delta = 0$$
$$Y_c^m(t) + \gamma = 0$$
$$X_c^e(t) + \alpha = 0$$
$$Y_c^e(t) + \beta = 0 \tag{12}$$

Contact C
$$X_c^m(t) - B_2 = 0$$
$$X_c^e(t) - MY_c^e(t) - B_1 = 0 \tag{13}$$

B. Task Decomposition

Fig. 3 depicts the anticipated progression of contacts during the insertion task. The operator first slides the peg toward the hole on the table surface. As the peg enters the hole, it first slides on one corner of the hole (contact state A). It then makes contact with both sides of the hole (contacts AB) and maintains these contacts until the bottom of the hole is reached (contacts BB'). Finally, it is placed flush with the right side of the hole (contacts CC') and released.
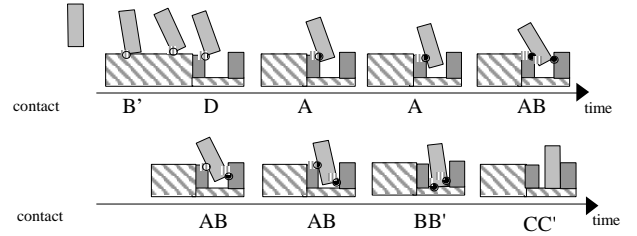

Fig. 3. Sequence of subtasks resulting from task decomposition.

As a means of testing the automatic segmentation procedure, the operator presses a switch during the task at each change of contact state. Peg position, velocity and angle are recorded at a rate of 50 Hz.

The goal of the identification procedure is to estimate the length and width of the peg as well as the location, axis and width of the hole. For the purposes of data segmentation, the task decomposition of (14) is assumed given.

$$\mathcal{T} = \begin{cases} \text{Carry} = \left(\{\emptyset\}, \{\emptyset\}\right), \\ \text{Slide toward hole} = \left(\{B'\}, \begin{Bmatrix} \text{peg length,} \\ \text{peg width,} \\ \text{hole axis} \end{Bmatrix}\right), \\ \text{1 - contact peg insertion} = \left(\{A\}, \{\text{hole corner}\}\right), \\ \text{2 - contact peg insertion} = \left(\{A, B\}, \begin{Bmatrix} \text{hole corner,} \\ \text{hole width} \end{Bmatrix}\right), \\ \text{Seat peg} = \left(\{B, B'\}, \{\emptyset\}\right), \\ \text{Insertion complete} = \left(\{C, C'\}, \{\emptyset\}\right), \\ \text{Release peg} = \left(\{\emptyset\}, \{\emptyset\}\right) \end{cases} \tag{14}$$

It consists of seven subtasks whose contact states are described by (9) and the specified subset of (10)-(13).

C. Data Segmentation

During data segmentation, position error between the master and remote manipulators is used to compute contact force. At the start of the task, vertical contact force is filtered and thresholded at -0.2 N to identify the end of the "Carry" subtask.

Once this condition is met, a 30-point sliding data window is used to test the multiple correlation coefficient (7) for successive subtasks. The contact sequence for a typical trial is shown in Fig. 4.
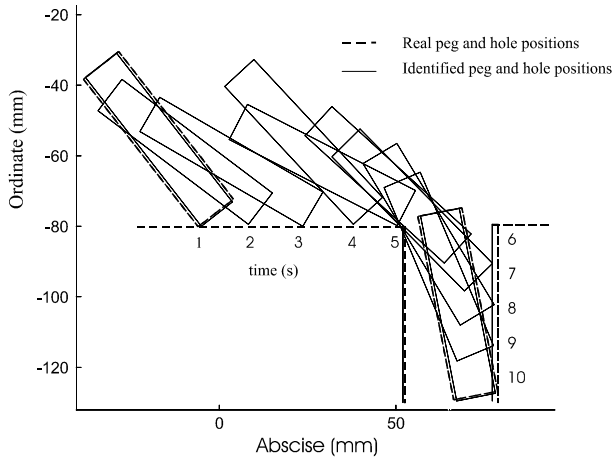

FIG. 4. Actual and estimated peg and hole locations. The peg is depicted at one second intervals during the insertion task.

Subtask 2, "Slide toward hole," corresponds to contact B'. Equations (9) and (11) can be expressed as

$$Y_i^{Tip} = \begin{bmatrix} X_i^{Tip} & 1 & -\sin\theta_i & -\cos\theta_i \end{bmatrix} \begin{bmatrix} M \\ B \\ \delta + M\gamma \\ \gamma - M\delta \end{bmatrix} \quad (15)$$

The results for a typical trial are shown in Fig. 5. During this subtask, hole axis and peg corner coordinates are estimated. Contact state B' is accepted as active when $R^2 \geq 0.99$. As a means of testing the statistical estimation technique, the operator presses a switch on the master's stylus to mark the beginning and end of this subtask.

Based on the depicted moving data window results for M, B, γ and δ, it can be seen that the automatic segmentation is superior to the switch-based segmentation. The latter (solid line segment) exhibits a time lag. Note that the second hatched segment between 6 and 8 seconds corresponds to the operator "accidentally" sliding the peg corner into the hole in a straight line. This segment is ignored as the segmentation routine has moved on to subtask 3 at this time.

Fig. 6 depicts the squared correlation coefficient and moving window estimates for the third subtask, "1-contact peg insertion." Equations (9) and (10) for contact A can be expressed as (16). For this subtask, automatic segmentation agrees well with manual segmentation in estimating the hole corner location.

$$Y_i^{Tip}\sin\theta_i + X_i^{Tip}\cos\theta_i + \delta = \begin{bmatrix} \cos\theta_i & \sin\theta_i \end{bmatrix}\begin{bmatrix} \alpha \\ \beta \end{bmatrix} \quad (16)$$
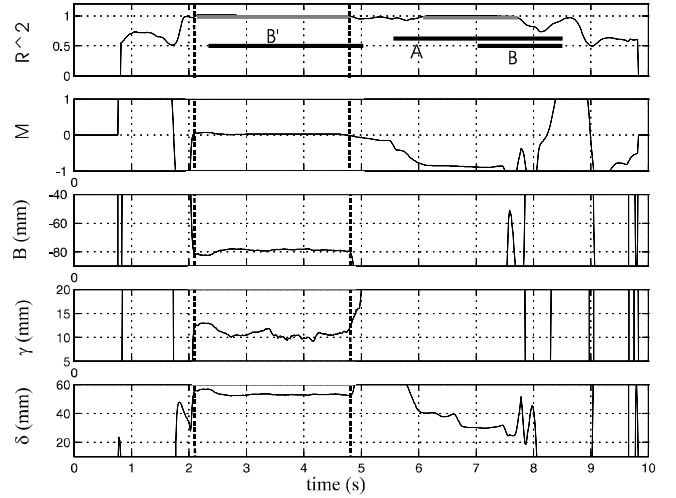

FIG. 5. Segmentation of subtask 2, "Slide toward hole". Contact state is B' corresponding to **(11)**. Hatched segment obtained using correlation coefficient. Solid segment corresponds to manual operator segmentation by switch.
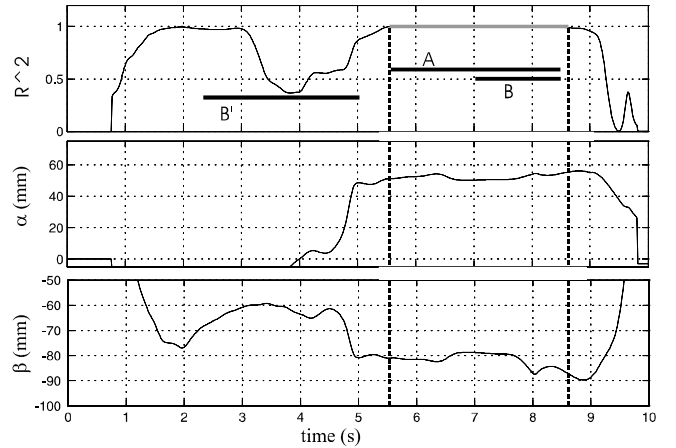

FIG. 6. Segmentation of subtask 3, "1-contact peg insertion". Contact state is A. See **(10).** Hatched segment obtained using correlation coefficient. Solid segment corresponds to manual operator segmentation by switch.

Subtask 4, "2-contact peg insertion," is the final property-estimating subtask. The contact state is $\{A,B\}$. At this point, all properties are estimated except hole width, which depends on ρ. The estimation equation is given by

$$\rho = \begin{bmatrix} X_i^{Tip} & Y_i^{Tip} & -\sin\theta_i & \cos\theta_i \end{bmatrix}\begin{bmatrix} 1 \\ -M \\ \gamma + M\delta \\ \delta - M\gamma \end{bmatrix} \quad (17)$$

Since ρ is the single unknown in (17), a correlation coefficient cannot be computed. Therefore, a threshold test on the

standard deviation, $\sigma(\rho) \le 0.8$, is used for automatic segmentation. Fig. 7 shows that this threshold is conservative in comparison to manual segmentation.
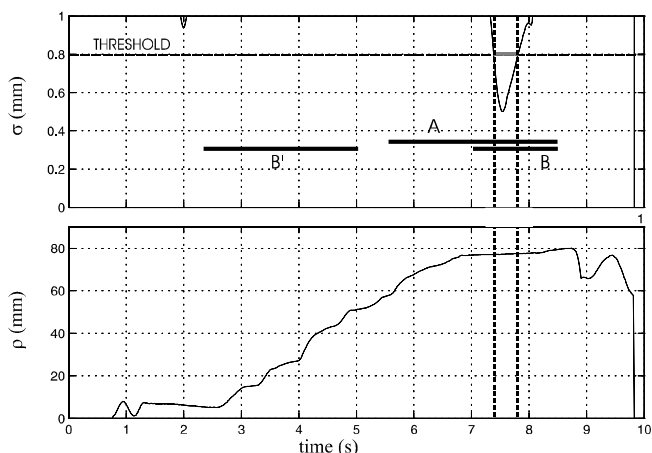

FIG. 7. Segmentation of subtask 4, "2-contact peg insertion". Contact state is $\{A, B\}$. Hatched segment denotes where standard deviation, σ, of **(17)** indicates contact B is active. Solid segment marks manual operator segmentation by switch.

Numerical comparisons of the estimated properties with direct measurements appear in Table 1. See Fig. 8 for a pictorial comparison.

Properties	Direct measurement	Estimated value
γ (peg width)	12.7 ±0.5 mm	11.2 ±1 mm
δ (peg length)	52.5 ± 0.5 mm	53.4 ±1 mm
M (table slope)	0± 0.1	0.03 ±0.5
B (table offset)	-80.0 ± 0.5 mm	-79.1± 1 mm
α (top-left hole corner x)	53.0 ± 0.5 mm	52.5 ±1 mm
β (top-left hole corner y)	-80.0 ± 0.5 mm	-81.08 ±1 mm
ρ (right side of hole, x)	80 ±0.5 mm	77.3 ±1 mm
$\rho - \alpha$ (hole width)	27.0± 0.5 mm	24.8 ± 1 mm

TABLE 1. COMPARISON OF ESTIMATED AND DIRECTLY MEASURED PROPERTY VALUES.

V. CONCLUSIONS

The preceding example has demonstrated that machine interpretation of the remote environment data stream can rival or exceed that of the operator. The proposed approach to contact state identification was clearly on a par with that of the operator. With regard to property estimation, it is apparent that the level of accuracy reflected in Table 1 far exceeds what could be achieved by the operator using visual and kinesthetic feedback.

Broad classes of environment identification problems require segmentation of data based on contact state. For those applications in which the contact states can be described by parameterized constraint equations, the proposed segmentation technique holds promise. Clearly, additional work is needed to extend the technique to more sophisticated phys-ics-based contact models which incorporate velocity and force data.

The advantages of the proposed approach provide ample motivation for doing so. In contrast to training-based statistical models, the current approach advocates the use of physical contact models. Furthermore, the approach offers the advantage that threshold values for accepting a particular contact state as valid are directly tied to a probability of false acceptance.

VI. REFERENCES

[1]   An, C., Atkeson, C., and Hollerbach, J. (1985). Estimation of Inertial Parameters of Rigid Body Links of Manipulators. *Proc. 24th Conference on Decision and Control*, Ft. Lauderdale, FL, December, 990-995.

[2]   Bruyninckx, H. (1995). Kinematic Models for Robot Compliant Motion with Identification of Uncertainties. Doctoral Dissertation, Department of Mechanical Engineering, Katholieke Universiteit Leuven, Belgium, April.

[3]   Delson, N. and West, H. (1996). Segmentation of Task Into Subtasks for Robot Programming by Human Demonstration. *ASME Japan/USA Symposium on Flexible Automation*, Boston, MA, 1, July, 41-47.

[4]   Driels, M. R. (1993). Using Passive End-Point Motion Constraints to Calibrate Robot Manipulators. *Transactions of the ASME*, 115, September, 560-566.

[5]   Dupont, P., Schulteis, T., and Howe, R. (1997). Experimental Identification of Kinematic Constraints. *Proceedings of the 1997 IEEE International Conference on Robotics and Automation*, Albuquerque, NM, April, 2677-2682.

[6]   Dupont, P., Schulteis, T., Millman, P and Howe, R. (1998). Automatic Identification of Environment Haptic Properties. *Prescence*, in review.

[7]   Eberman, B. (1997). A model-based approach to Cartesian manipulation contact sensing. *International Journal of Robotics Research,* (16)4, August, 508-528.

[8]   Fiorini, P., Losito, S., Giancaspro, A., and Pasquariello, G. (1992). Neural Networks for Off-line Segmentation of Teleoperation Tasks. *Proceedings of the 1992 IEEE International Symposium on Intelligent Control*, Glasgow, UK, 1, August, 17-22.

[9]   Griebenow, B.E. (1994). Buried-waste Integrated Demonstration Retrieval Projects. Annual Meeting of American Nuclear Society, New Orleans, LA, 19-23 June, *Trans. Am. Nucl. Soc.*, 70, 402.

[10]   Hannaford, B., and Lee, P. (1991).Hidden Markov Modal Analysis of Force/Torque Information in Telemanipulation. *International Journal of Robotics Research*, 10(5), October, 528-539.

[11]   Leahy, M. B., Jr. and Hamill, N. (1995). The Next Generation Munitions Handler Prototype Acquisition Campaign: Targets \& Courses of Action. Research Paper, ACSC/DEA/205/05-05, Air Command and Staff College.

[12]   Lin, S. T., and Yae, K. H. (1992). Identification of Unknown Payload and Environmental Parameters for Robot Compliant Motion" *Proceedings of the 1992 American Control Conference*, Chicago, 4, June, 2952-2956.

[13]   MacLean, K. (1996). The `Haptic Camera': A Technique for Characterizing and Playing Back Haptic Properties of Real Environments. *Proceedings of the ASME Dynamic Systems and Control Division*, Atlanta, GA, DSC-58, November, 459-467.

[14]   McCarragher, B. J., 1994(a), Force Sensing from Human Demonstration Using a Hybrid Dynamical Model and Qualitative Reasoning. *Proceedings of the 1994 IEEE Conference on Robotics and Automation*, 1, May, 557-563.

[15]   McCarragher, B. J., 1994(b), Petri Net Modeling for Robotic Assembly and Trajectory Planning. *IEEE Transactions on Industrial Electronics*, 41(6), December, 631-640.

[16]   Pook, P. K., and Ballard, D. H. (1993). Recognizing Teleoperated Manipulations. *Proceedings of the IEEE International Conference on Robotics and Automation*, 2, May, 578-585.

[17]   Satava, R., and Jones, S. (1997). Virtual Environments for Medical Training and Education. *Presence*, 6(2), April, 139-146.